Michael Dreyer ORCID iD: 0000-0002-5511-4983

José I. Contreras Raggio ORCID iD: 0000-0002-7457-9559

William Taylor ORCID iD: 0000-0003-4060-4098

The influence of implant design and limb alignment on *in vivo* wear rates of fixed-bearing and rotating-platform knee implant retrievals

Michael J. Dreyer[1,2], Bernhard Weisse[2], José Ignacio Contreras Raggio[2,3], Robert Zboray[4], William R. Taylor[1,*], Stefan Preiss[5], Nils Horn[5]

[1] Laboratory for Movement Biomechanics, Institute for Biomechanics, ETH Zürich, Zürich, Switzerland

[2] Laboratory for Mechanical Systems Engineering, Empa, Dübendorf, Switzerland

[3] Facultad de Ingeniería y Ciencias, Universidad Adolfo Ibáñez, Padre Hurtado 750, Viña del Mar, Chile

[4] Center for X-ray Analytics, Empa, Dübendorf, Switzerland

[5] Department of Lower Extremities, Schulthess Clinic, Zürich, Switzerland

*corresponding author

Correspondence FOR PRINT VERSION:

William R. Taylor
Gloriastrasse 37/39
8092 Zürich
Switzerland
bt@ethz.ch

Correspondence DURING REVIEW:

Michael Dreyer
Gloriastrasse 37/39
8092 Zürich
Switzerland
michael.dreyer@hest.ethz.ch

This article has been accepted for publication and undergone full peer review but has not been through the copyediting, typesetting, pagination and proofreading process, which may lead to differences between this version and the Version of Record. Please cite this article as doi: 10.1002/jor.25734.

Running title: Effects on Knee Implant Wear

Keywords: knee implant; wear; arthroplasty; retrievals; 3D scanning

Word count: 4029

Author Contributions:

Conceptualization: MJD, WRT. Data curation: MJD, RZ, NH. Formal analysis: MJD. Funding acquisition: BW, SP, WRT. Investigation: MJD, JICR. Methodology: MJD. Project administration: MJD, BW. Resources: BW, RZ, SP. Software: MJD. Supervision: BW. Validation: MJD, JICR. Visualization: MJD. Writing – original draft: MJD. Writing – review & editing: MJD, BW, WRT, NH.

All authors have read and approved the final submitted manuscript.

Abstract

Analysis of polyethylene wear in knee implants is crucial for understanding the factors leading to revision in total knee arthroplasty. Importantly, current experimental and computational methods for predicting insert wear can only be validated against true *in vivo* measurements from retrievals. This study quantitatively investigated *in vivo* polyethylene wear rates in fixed-bearing (n=21) and rotating-platform (n=53) implant retrievals. 3D surface geometry of the retrievals was measured using a structured light scanner. Then, a reference surface that included the deformation, but not the wear that the retrievals had experienced *in vivo*, was constructed using a fully automatic surface reconstruction algorithm. Finally, wear volume was calculated from the deviation between the worn and reconstructed surfaces. The measurement and analysis techniques were validated and the algorithm was found to produce errors of only 0.2% relative to the component volumes. In addition to quantifying cohort-level wear rates, the effect of

mechanical axis limb alignment on mediolateral wear distribution was examined for a subset of the retrievals (n=14+26). Our results show that fixed-bearing implants produce significantly (p=0.04) higher topside wear rates (24.6±10.1 mm^3/year) than rotating-platform implants (15.3±8.0 mm^3/year). This effect was larger than that of limb alignment, which had a smaller and non-significant influence on overall wear rates (+4.5±11.6 mm^3/year, p=0.43). However, increased varus alignment was associated significantly with greater medial compartment wear in both the fixed-bearing and rotating-platform designs (+1.7±1.3 %/° and +1.8±1.6 %/°). Our findings emphasize the importance of implant design and limb alignment on wear outcomes, providing reference data for improving implant performance and longevity.

Introduction

Investigating polyethylene (PE) wear in knee implants is critical for our understanding of factors necessitating revision knee arthroplasty, as wear is known to play a key role in complications such as aseptic loosening and osteolysis[1,2]. Wear analysis is also necessary for assessing the impact of variables such as implant design, limb alignment, and component malpositioning on long-term implant survival. However, laboratory tests often fail to accurately reproduce the depth[3] and broad extent of wear scars[3–6], as well as the diversity of damage modes[4,7,8] observed *in vivo*. While computational models can offer predictive insights for data from large patient cohorts, provided realistic input loads and kinematics are even available, such models critically require extensive validation from experimental[9] or retrieval[10] studies to be credible. Therefore, whether the objective

is to investigate *in vivo* wear directly or to validate experiments and models, the need for real-world data from retrievals is unavoidable.

Retrieval-based wear quantification offers a realistic and credible approach to investigate wear-related failures. Here, the main quantity of interest is the volume (in mm^3) of particles removed from the PE inlays due to its correlation with osteolysis[11]. Volume, however, is a challenging quantity to measure in practice. Historically, retrieval damage has often been evaluated qualitatively using e.g. Hood scores[12], a manual grading system that lacks the capacity to directly convert to wear volume. More quantitatively, minimum inlay thickness has been measured using calipers[13], coordinate measuring machines[14], or µCT[15], and has been taken as a surrogate measure of wear and creep damage. However, the location of minimum thickness does not necessarily coincide with the location of maximum wear damage[14]. Even if it did, wear depth itself is only a moderate predictor of wear volume[16] since factors such as creep[17] and manufacturing tolerances[18] can influence such measurements. Similarly, quantification of the worn surface area obtained from e.g. image analysis, likewise does not correlate with wear volume[14]. Unfortunately, the simple approach of quantifying wear volume through gravimetric measurements[19] is also impossible for retrievals, as the pre-implantation weight of each specimen is generally unknown and manufacturing tolerances would introduce prohibitively large errors in any comparison to different unworn specimens[18] or the nominal CAD geometry[20].

Surface reconstruction emerges as a promising technique to quantify knee implant wear volumes. Here, the 3D geometry of the worn retrieval surface is measured, typically using optical or µCT systems. The original unworn surface is then reconstructed by

manually or automatically fitting either a polynomial or spline surface[21–24] or a design-congruent surface[10,14,25] to the unworn regions of the retrievals' surface. Finally, wear is calculated as the volume difference between the worn and reconstructed unworn surfaces. Thus, manufacturing tolerances and plastic deformation are elegantly excluded from the calculation of wear damage.

Using these surface reconstruction techniques, a number of clinically relevant questions on what parameters play a role on *in vivo* wear outcomes can be investigated. For instance, the impact of limb alignment on wear has been evaluated, with varus alignment >3° being associated with increased medial wear[15,26]. Moreover, a dependence on implant component orientation has been found[24]. Surprisingly, it has also been observed that despite their much greater backside sliding, rotating platform implants with a polished tibial tray produce less wear *in vivo* than fixed-bearing implants with very little backside motion, but a rough tray[27,28]. Currently, however, there is a critical lack of studies quantifying the relative importance of such factors driving wear volume outcomes in individuals.

The aim of our study was therefore to provide a quantitative evaluation of *in vivo* wear between two implant designs combined with a range of mechanical axis limb alignments to allow a comparison of the relative importance of these two parameters. Specifically, this was the first study performing surface reconstruction on both fixed-bearing (FB) and rotating platform (RP) retrievals, calculating population-level wear rates and furthermore investigating the relationship between mediolateral wear distribution and coronal plane limb alignment.

Methods

In this retrospective observational study (Level III evidence), we obtained FB and RP retrievals from two sources, measured 3D surface geometry using a structured light scanner, and calculated wear using a verified surface reconstruction technique.

Retrieval cohort

Institutional approval for this study was obtained from the ETH Zurich Ethics Commission.

Twenty-one revision-retrieved cruciate sacrificing FB Innex FIXUC (Zimmer Biomet, Zug, Switzerland) and 53 cruciate sacrificing mobile-bearing RP Innex UCOR (Zimmer Biomet) tibial inserts with a previous *in situ* time ≥ 1 year were obtained from a clinic (Schulthess Clinic, Zurich, Switzerland) and from the manufacturer (Zimmer Biomet). Both implant designs are ultra-congruent total knee replacements consisting of a polished cobalt-chromium femoral component, a tibial insert made of conventional ultra-high-molecular-weight-polyethylene (UHMWPE) gamma irradiated under nitrogen atmosphere, and a sand-blasted (FB) or polished (RP) cobalt-chromium tibial tray.

Additional data collected included the specific size and side (R/L) of the implant components, patient age at revision, time *in situ* of the insert prior to revision, hip-knee-ankle angle based on pre-revision coronal plane radiographs, and reasons for revision (Table 1). However, not all these data were available for all retrievals. The average patient age at revision was 68 years (range 50–91), with inserts retrieved an average 3.1

(range 1.0–9.4) years after primary implantation, mainly due to aseptic loosening (47%), pain (24%), instability (22%), hot patella (12%) [29], or infection (9%).

Table 1. Summary of patient demographics and retrieval cases. Limb alignment was deemed neutral if it was between -3° and 3°. Some specimens had multiple reasons for revision listed, which is why the percentages do not add up to 100% and why no percentage is given for "Others".

	Fixed bearing (Innex FIXUC)	**Rotating platform (Innex UCOR)**
Number of retrievals	21	53
Mean age at revision (range)	74 (61–91)	66 (50–79)
Mean years *in situ* (range)	3.2 (1.3–7.2)	3.1 (1.0–9.4)
Side L: R (: unknown)	13: 7 (: 1)	16: 34 (: 3)
Sex M: F (: unknown)	5: 15 (: 1)	14: 38 (: 1)
Alignment varus: neutral: valgus (: unknown)	6: 8: 0 (: 7)	3: 16: 7 (: 27)
Revision reasons		
Aseptic loosening	10 (48%)	25 (47%)
Pain	4 (19%)	14 (26%)
Instability	3 (14%)	13 (25%)
Hot Patella	3 (14%)	6 (11%)
Infection	1 (5%)	6 (11%)
Extensor Mechanism Deficiency	1 (5%)	3 (6%)
Periprosthetic fracture	3 (14%)	0
Others	7	15

3D scanning

3D surface geometries of the retrievals were obtained using a structured light 3D scanner (Pro S3, HP Inc., Palo Alto, USA) with a resolution of approximately 50µm. The device projects black-and-white light patterns onto the measured object while a camera arranged at a ~25° angle to the projector then records the patterns, which appear distorted based on the object's geometry (Figure 1). From this, the 3D-shape of the object's surface is reconstructed. Because reflections occurring on the glossy surface of the UHMWPE

retrievals would interfere with this process, prior to scanning, each retrieval was coated with a matte chalk spray (Laser Scanning Entspiegelungsspray, Helling GmbH, Heidgraben, Germany) to eliminate reflections. This chalk spray was found to produce a coating with a thickness of 13±7 µm (mean±SD) [30].

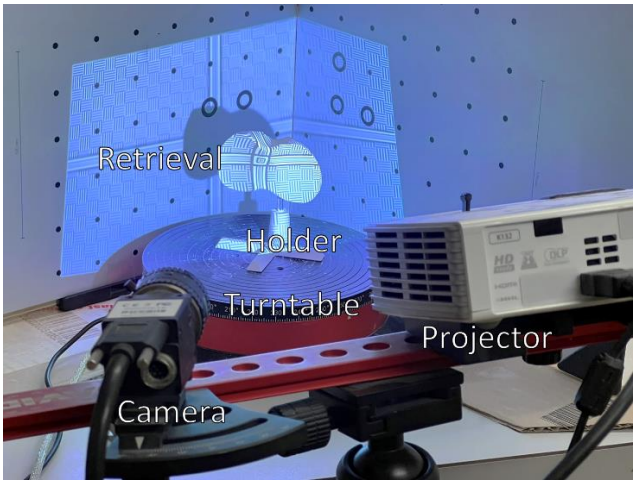

Figure 1. 3D scanning setup and components

The scanning process involved affixing the retrieval to a custom-made specimen holder with its anterior axis pointing upwards, placing it on an automatic rotating turntable and acquiring 36 scans, each at 10° intervals. An additional 36 scans were acquired after rotating the retrieval by 90° around its superior axis to capture all its sides. These 72 scans were then merged using the manufacturer's software to obtain a complete 3D-scan of the retrieval surface.

Surface reconstruction

Geometry and dimensions of retrieved inserts are affected by manufacturing tolerances[18,20,27], plastic deformation[17,19], and the applied coating[30,31]. To reliably measure

wear despite these sources of error, we here employ a surface reconstruction technique where the unworn retrieval geometry was reconstructed from a design-congruent surface[23]. As obtaining unworn physical specimens for each combination of insert design, size, and thickness in the retrieved cohort was not possible, we here used the size-matched nominal CAD geometry of each individual insert as the reference geometry and surface, which were registered to unworn insert regions. The fully automatic surface reconstruction algorithm (Figure 2) was implemented in Python 3.7 using the Open3D library[32].

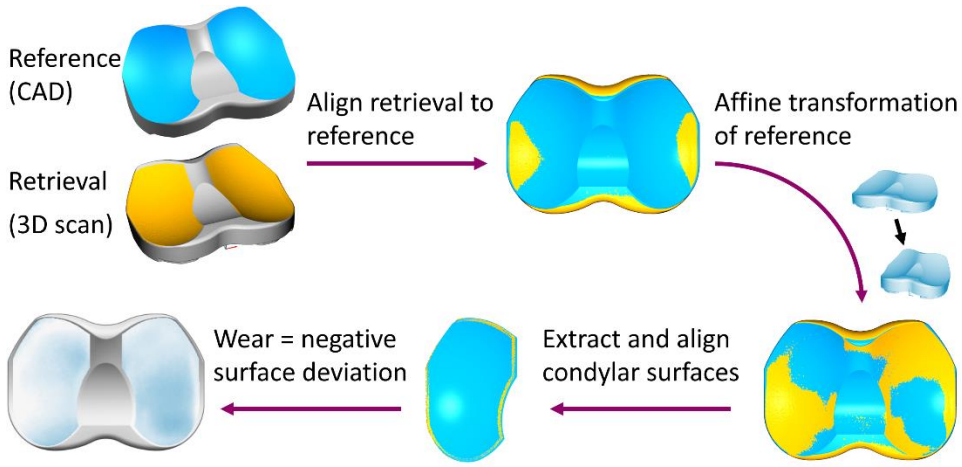

Figure 2. Surface reconstruction algorithm to obtain topside wear from 3D scans of knee implant retrievals.

In the first step of our algorithm, the whole scan of the retrieval was randomly positioned in space, coarsely aligned to the reference using a fast global registration algorithm, and finely aligned using an iterative-closest-point algorithm.

To further improve alignment and to account for manufacturing tolerances, coating thickness, and global creep deformations experienced *in situ* that affected the whole specimen, the reference geometry was registered to the scan using an affine

transformation where the reference was scaled and skewed individually along each of the anterior-posterior (AP), medio-lateral (ML), and superior-inferior (SI) axes, minimizing its deviation from the retrieval scan. With this affine transform, we aimed to subject the reference to the same manufacturing tolerances and creep deformation that the retrieval had experienced *in vivo*, thus minimizing these sourceso of surface deviations from subsequent wear calculations.

Then, the medial and lateral condylar articulating surfaces were extracted from the deformed reference and from the scan. Lastly, the reference's condylar surfaces were fitted to a 1mm thick strip around the outer boundary of the scan condyles, assuming there would be little to no wear at the outer rim of the retrievals. With the condylar surfaces thus reconstructed on the scan, the difference in superior-inferior direction between the scan and reconstructed surfaces was calculated at each point on the surface, with negative deviations indicating wear.

Due to imperfect alignment and local deformation of the retrievals, positive deviations, i.e. the scan laying outside of the reference surface, could occur at unspecified locations. In reality, material could not have actually been added to the retrievals, but positive deviations would result in reduced wear results. Similar to a previous study, we minimized the associated error by setting any positive deviation to zero[27]. Finally, total topside wear volume was calculated by integrating over the negative surface deviations on each condyle and summing the medial and lateral contributions.

It should be noted that quantification of wear on the backside of the retrievals was not possible using the approaches proposed. As the whole backside is in contact, it

potentially experiences wear everywhere on its flat surface, and, as such, does not offer an unworn region that could be utilized for surface reconstruction. Therefore, this study presents a comparison of topside insert wear only.

Validation

3D scanning

The 3D optical scanner employed in this study was slightly less accurate than modern µCT scanners. Studies using similar laser-scanning techniques have demonstrated that optically-derived surfaces vary from and produce larger volumes than objects measured using µCT[31]. Thus, to validate our measurement setup, we performed µCT measurements (EasyTom XL, RX Solutions, Chavanod, France) on three of the FB retrievals and compared them to the corresponding 3D scans to quantify surface variations. Specifically, for each of the three chosen retrievals, the 3D scan was registered to the µCT scan using an iterative closest point algorithm and the local mesh-to-mesh distance was calculated at each point of the mesh using the open source software CloudCompare V2.12.

Surface reconstruction algorithm

To verify the surface reconstruction algorithm, we applied it to virtual retrievals. A virtual retrieval here denotes a scan of an unworn insert of known volume, that we then deformed and/or applied virtual surface indentations to, using 3D modelling software, in order to mimic the damage patterns commonly observed in retrievals. Since the volume before and after applying wear damage was known, the virtual retrievals provided a baseline amount of wear against which we could compare the results of our algorithm.

Eight virtual retrievals based on two scans of unworn FB inserts (#1 and #2) were generated (Table 2) and the root-mean-square-error (RMSE) of the surface reconstruction relative to the baseline was evaluated.

Table 2. Virtual retrievals that were created based on scans of unworn inserts to verify the surface reconstruction algorithm.

#	Type of deformation	Type of damage (max. depth)
1a	None	None
1b	None	Wear (-0.34 mm)
1c	None	Wear (-0.14 mm)
2a	None	None
2b	None	Wear (-0.14 mm)
2c	None	Wear (-0.36 mm)
2d	Scale +1% AP and -1% ML	None
2e	Scale +1% AP and -1% ML	Wear (-0.48 mm)

Statistical analysis

Statistical analyses of the effects of implant design and limb alignment on wear volumes were conducted in R[33].

As limb alignment information was available only for 14 (67%) FB and 26 (49%) RP retrievals, we initially left this parameter out of the analysis and investigated only the effect of design on cohort-level wear rates. Specifically, a multiple linear regression model was fitted to the entire dataset for 74 retrievals, with interaction terms included to account for potential differences in the effect of the time *in situ* on the wear volume between the two groups. The model was defined as:

$$v_{wear} \sim \beta_0 + \beta_1 t_{years} + \beta_2 t_{years} D_{group}$$

where v_{wear} represented the total wear volume in mm³, t_{years}, the independent variable, represented the years *in situ*, and D_{group} represented the design group of each observation. The intercept term β_0 represented any positive error introduced in the surface reconstruction algorithm by considering only negative surface deviations. The slope of the regression line β_1 represented the wear rate of one design in mm³/year, as in previous works[23,25], while β_2 represented the additional wear rate of the other design. The same model was fitted to the sub-cohort of 40 retrievals to check whether there would be significant differences in wear rates due to a reduction in cohort size.

Finally, the combined influence of limb alignment and implant design was investigated through an extension of the initial model, defined as:

$$v_{wear} \sim \beta_0 + \beta_1 t_{years} + \beta_2 t_{years} D_{group} + \beta_3 t_{years} L_{alignment}$$

Here, $L_{alignment}$ represented the limb alignment in categories valgus, neutral, or varus, while β_3 represented the difference in wear rates between neutral, varus, and valgus alignments.

Additionally, to investigate the impact of limb alignment on wear distribution on the insert, we defined the mediolateral wear ratio as the wear volume on the medial condyle divided by the total wear volume across both condyles for each specimen[34]. Then, we once more performed a multiple linear regression on the data for the medial wear ratio m_{ratio} over the varus angle v_{angle} (in °) for the sub-cohort with alignment data:

$$m_{ratio} \sim \gamma_0 + \gamma_1 D_{group} + \gamma_2 v_{angle} + \gamma_3 v_{angle} D_{group}$$

The terms γ_0 and $\gamma_1 D_{group}$ represent the wear distribution for a neutral (0°) alignment of each design, while $\gamma_2 v_{angle}$ and $\gamma_3 v_{angle} D_{group}$ represent the change in wear distribution caused by a change in limb alignment.

For all models, significance was defined at a p-value of 0.05.

Results

Validation

3D scanning

The 3D-scanned surfaces lay mostly outside of the μCT surfaces with an average deviation of +40±48 μm (mean±SD) and 5th–95th percentile range of -37 – 115 μm (Figure 3). The volume of the 3D-scanned specimens was +398±138 mm³ (mean±SD) larger, which was equivalent to 1.7±0.6% (mean±SD) of the total insert volume.

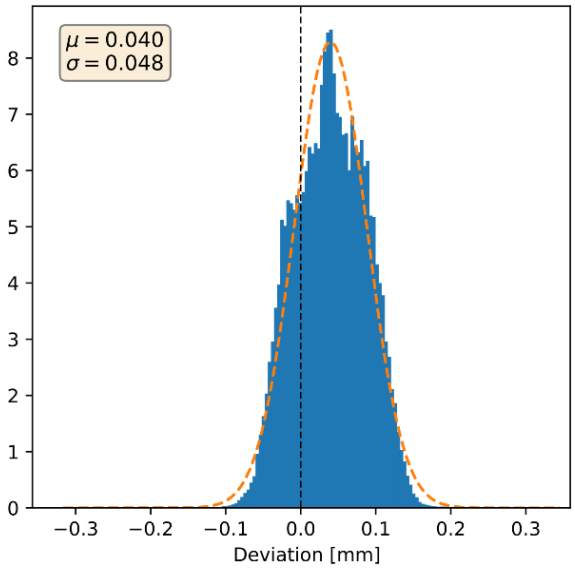

Figure 3. Histogram (blue) of the mesh-to-mesh distances of all three checked specimens as well as mean (μ) and standard deviation (σ) of the associated normal distribution (orange). Positive deviations indicate the 3D scan geometry lying outside the μCT geometry.

Surface reconstruction algorithm

The surface reconstruction algorithm slightly overestimated the amount of wear on the virtual retrievals, even for the three cases where the virtual retrievals experienced 0 mm^3 actual wear damage (Figure 4). The range of errors across all virtual retrievals was 0–35 mm^3 and the RMSE was 23 mm^3.

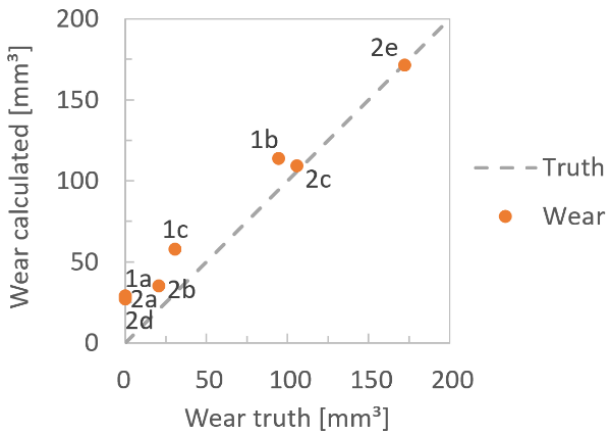

Figure 4. Wear volume calculated by the surface reconstruction algorithm plotted over the ground truth wear volume for the eight virtual retrievals. Data points lying above the "Truth" line indicate an overestimation of wear by the algorithm. The annotations ("1a", "1b", etc.) correspond to those in Table 2. The overall root-mean-square-error was 23 mm^3.

Retrievals

Global deformations

In an effort to reflect global deformation that the retrievals likely experienced *in situ*, the reference geometries were nonuniformly scaled during the surface registration procedure. Along the AP, ML, and SI axes, the mean deformations were small, ranging between -1.4 – 1.2% across groups and directions (Figure 5), with a few outliers skewing the distributions positively along the AP and negatively along the ML axes.

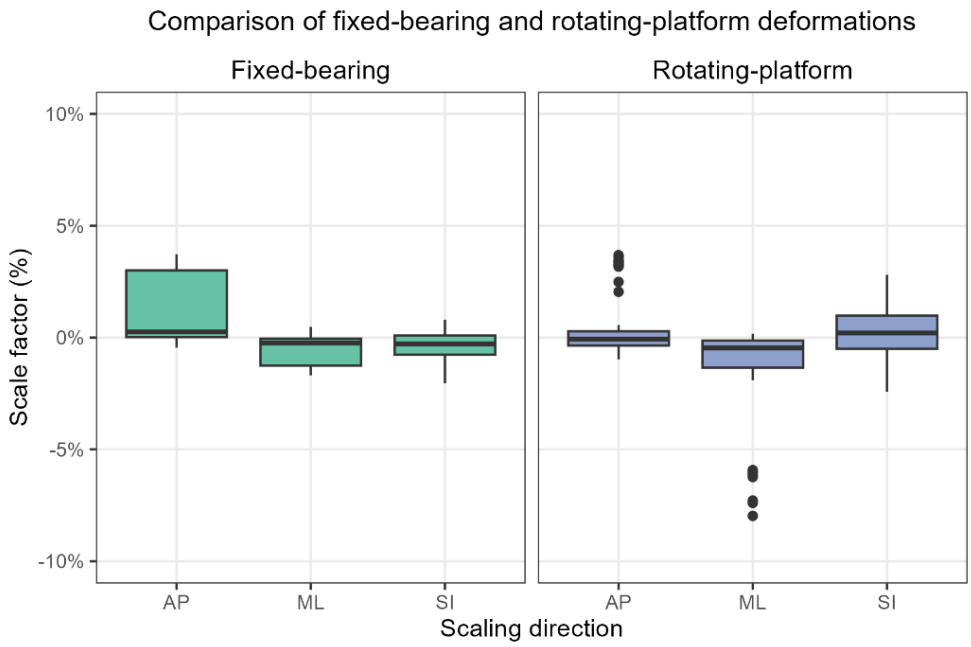

Figure 5. Boxplots of the deformation of the retrievals in the anterior-posterior (AP), medial-lateral (ML), and superior-inferior (SI) directions for the two implant designs relative to the reference CAD geometries. Black dots indicate outliers.

Wear maps

Based on the comparison of the retrieval and the reconstructed surfaces, wear damage was clearly visible from the generated surface deviation maps, especially for inserts with multiple years *in situ*. Based on a visual investigation of the individual and average surface deviation plots (Figure 6a), there seemed to be a trend for the FB retrievals of wear occurring anteriorly on the medial condyle and posteriorly on the lateral condyle, while no such trend could be observed on the RP retrievals. Furthermore, eight of the most deformed RP retrievals (all of them outliers with respect to deformation, Figure 5) showed surface deviation maps where no wear, but just an overall mismatch in surface shape was apparent (Figure 6b).

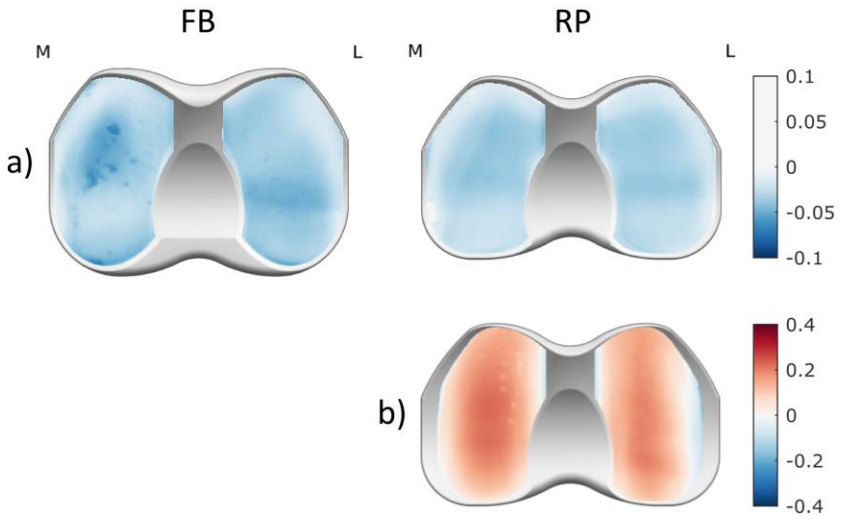

Figure 6. Surface deviation plots showing wear damage. a) The mean wear of the fixed-bearing (FB) and rotating-platform (RP) retrievals after scaling each individual surface deviation map to that of a medium-sized insert. Only negative deviations are plotted in accordance with the employed surface reconstruction algorithm that sets positive deviations to zero (white) before calculating the wear (blue) volume. b) A strongly deformed RP specimen. Negative values (blue) are interpreted as wear while positive values (red) are interpreted as errors.

The maximum wear depth on each specimen for the FB and RP groups had mean values of 0.33 mm (range: 0.21–0.58 mm) and 0.37 mm (range: 0.11–0.84 mm), respectively. No significant relationship between wear depth and wear volume (see below) or implant design was observed.

Effect of implant design on wear rates

Based on the surface deviation maps, wear volumes and rates were calculated. In the full-cohort analysis without limb alignment effects, wear rates (±95% CI) were 24.6±10.1 mm^3/year ($p<0.001$) for the FB design and a lower 15.3±8.0 mm^3/year ($p<0.001$) for the RP design (Figure 7). While these values did meet our criterion for significance, both design groups showed considerable variability of the wear volumes, even after short durations *in situ*, which is reflected in the relatively large CIs, as well as in the R^2 values

of 0.37 and 0.19, respectively. Still, the difference in wear rate between the FB and RP designs was significant (p=0.04).

The intercept (±95% CI) at 0 years was 35.1±28.1 mm^3, was significantly different from zero (p=0.02), encompassed the range and RMSE of errors associated with the analysis technique as determined within the virtual retrievals validation (Figure 4).

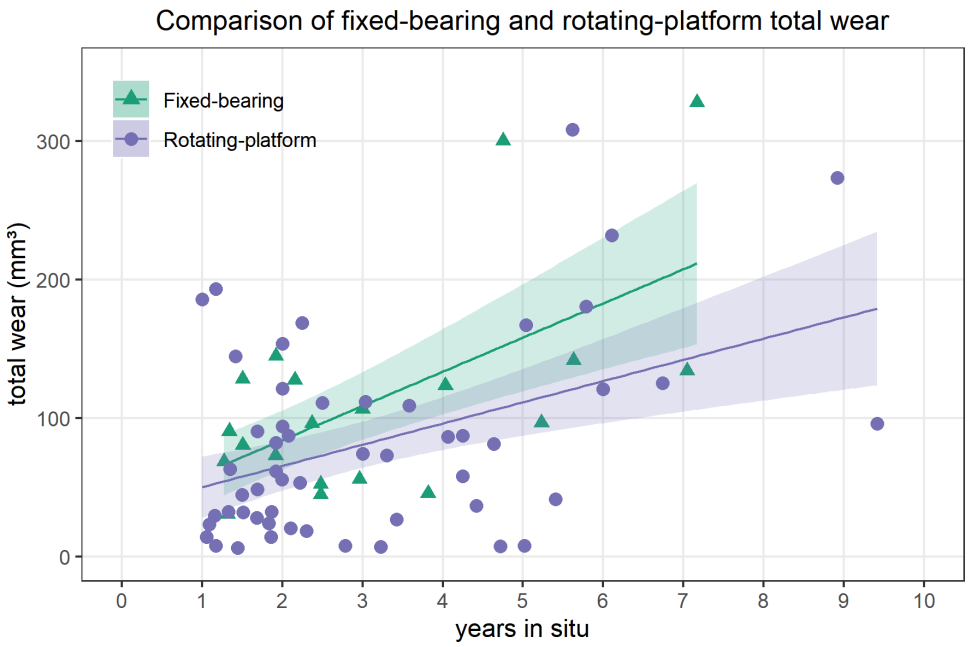

Figure 7. Topside wear volume as a function of time *in situ* for the fixed-bearing and rotating-platform groups. The lines represent the linear regressions, while the shaded areas represent the 95% confidence intervals. Complete data for the full cohort are shown, i.e. the effect of mechanical axis limb alignment is not presented.

Effect of limb alignment on wear rates and distribution

Fitting the same model to the sub-cohort for which limb alignment information was available yielded wear rates that were not significantly different from those for the full cohort, but did not show a significant difference between the two designs anymore.

After the effect of limb alignment was added to the regression model, the wear rates for the FB and RP sub-cohorts with limb alignment were 11% (27.3±12.6 mm^3/year) and 15% (22.4±10.0 mm^3/year) higher than for the full cohorts, but these differences were not significant. The intercept was -1.4±37.7 mm^3 (p=0.93). Compared to neutral alignment, there was no significant effect of varus alignment (+4.5±11.6 mm^3/year, p=0.43) or valgus alignment (-7.4±13.9 mm^3/year, p=0.28) on total wear rates.

Generally, 27–84% of overall wear occurred on the medial condyle for the FB subjects for the sub-cohort with alignment data, while 11–84% was observed for the RP subjects. For straight limb alignment of 0° (i.e. at the intercept), the proportion of medial condyle wear (±95% CI) predicted by the regression model was 42.0±9.6% (p<0.001) for the FB and 44.4±6.2% (p<0.001) for the RP design (Figure 8). The relative amount of medial wear increased with increasing varus angle for both the FB design (at a rate of 1.7±1.3 %/°, p=0.01) and the for RP design (1.8±1.6 %/°, p=0.03). Comparison between the two design groups yielded no significant differences for the distribution at neutral alignment, i.e. the intercept (p=0.67), and for the effect of increased varus, i.e. the slopes (p=0.87).

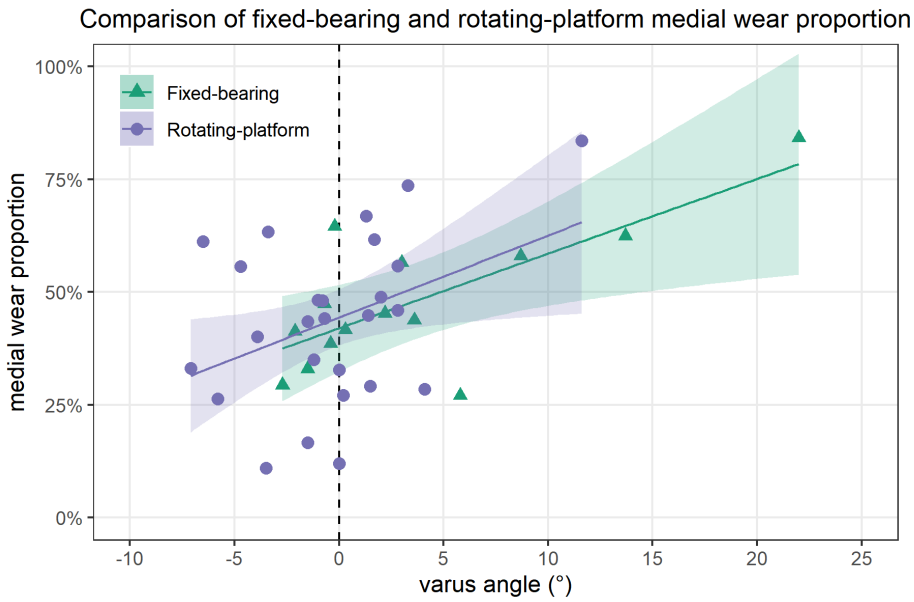

Figure 8. Ratio of medial condyle wear to overall wear as a function of limb alignment (varus) angle for the fixed-bearing and rotating-platform groups. The lines represent the linear regressions, while the shaded areas represent the 95% confidence intervals.

Discussion

In this study, we aimed to accurately quantify *in vivo* wear rates for fixed-bearing and rotating-platform knee implants to investigate the relative importance of implant design and mechanical axis limb alignment on clinical wear outcomes. We found that the effect of implant design on the topside wear rate was significant and larger than the non-significant effect of limb alignment. Specifically, RP designs experienced 39% lower wear rates *in vivo* than FB designs, hence offering increased implant longevity, especially benefitting young active patients[35]. This effect was larger than that observed for limb alignment, which had no significant effect on overall wear rates, even though alignment was shown to affect the mediolateral distribution of wear that did occur. A balanced wear distribution was demonstrated at neutral to slight varus limb alignment, which is consistent with current surgical practice for primary implantation where surgeons generally target a 0–3° varus alignment at the knee.

To arrive at these conclusions, we employed 3D scanning and surface reconstruction techniques to quantify cohort-level wear rates on the topside surfaces of 74 retrievals (mean 3.1 years *in situ*). The accuracy and precision of the 3D scanner used here (+40±48 μm, mean±SD) were comparable to that of a similar study using laser scanning (+71±36 μm [31]), which also necessitates the application of a matt coating to the retrievals. Our machine produced 1.7±0.6% (mean±SD) larger insert volumes than the baseline μCT measurements, plausibly due to the additional coating, which is consistent with the literature[31]. However, any uniform thickening of the retrieval surface would have been compensated in our algorithm by the affine transform introduced here, which allowed scaling in all directions. In fact, the RMSE of the surface registration algorithm of only 23 mm^3, or 0.1% of the specimen volume, was considerably smaller than both the specimen volume error after 3D scanning of 1.7% and the maximum observed wear volume of 328 mm^3. These findings lend initial credibility to the surface reconstruction algorithm, which refines upon previous such algorithms by being fully automated and including an affine transformation to minimize the presence of creep and manufacturing tolerances in the results.

The most appropriate comparisons for our results are other studies that used surface reconstruction techniques. For the FB implant, we found a wear rate of 25±10 mm^3/year (±95% CI), which was not significantly different from previously published FB implant wear rates obtained from surface reconstruction of 12±5 mm^3/year [24], 13±6 mm^3/year [14], 16±8 mm^3/year [10], and 17±23 mm^3/year [36]. Little wear data has been published specifically for the Innex implants, for which a wealth of loading and kinematic data is publicly available[37]. In a previous wear model validation study[9] against *in vitro* simulator

experiments performed on the Innex FB implant using standardized level walking input conditions[38], we found similar wear patterns but a wear rate of 4.8 mm^3/year (assuming 1.1 million cycles/year[39]), which is approximately five times smaller than the *in situ* data reported here. The higher wear rates observed *in vivo* clearly demonstrate the more varied and aggressive modes of damage *in situ*, including wear but also PE aging and pitting, which are challenging to predict computationally or experimentally, but should be addressed in future investigations. Our observed large inter-subject variations in wear outcomes produced R^2 values of 0.19 and 0.37 of the linear fits to the wear volume over time, which is not unusual compared to previous retrieval studies[10,14,24,25,36] reporting R^2 values in the range of 0.19–0.41.

We are not aware of other studies that applied surface reconstruction methods to measure wear volumes of RP retrievals. In our study we found an estimated topside wear rate of 15.3±8.0 mm^3/year (±95% CI) for the RP inserts, which was significantly lower (39%) than for the FB design. It is likely that even if backside wear was included, RP wear would not exceed FB wear[40]. In fact, some previous retrieval[27] and experimental[28] studies found lower total, and even backside, wear rates for RP than FB implants. These studies, like ours, compared RP implants with polished tibial trays to FB implants with rough tibial trays, which likely increases wear[41–43]. As we did not include backside wear in our study, the observed significant differences between the designs possibly indicate more severe topside conditions in FB implants. Moreover, qualitative differences were found for wear scar location, with the FB implants showing asymmetric locations on the two condyles, while the RP implants showed no discernible differences in wear location between the condyles. This is in line with a previous study comparing surface deviations

between FB and RP retrievals[44]. These differences can be explained by the RP design, where the rotational freedom of the insert mediates alignment to the femoral component, hence reducing stress and wear on the PE insert[45], even though this mechanism also potentially leads to a higher risk of instability (11% more in Table 1) and spin-out[46].

A limb alignment with >3° varus was only weakly (p=0.43) associated with increased wear compared to neutral and valgus alignment. However, the proportion of medial condyle wear significantly increased with increasing varus. This is likely due to the increased medial loading with increasing varus, as observed in previous computational[47,48] and experimental[49] studies. It also matches previous retrieval studies, where varus alignment was found to be correlated with medially and overall increased stress, wear, and damage[15,26,34,50].

Limitations

The biggest limitation of this study was that backside wear could not be analyzed, meaning we could not quantify wear on the whole retrievals. A second limitation is that retrievals from revision surgery represent failed specimens, which may introduce some bias compared to successful cases where no revision surgery is necessary and the wear generally can only be quantified posthumously. However, a previous study found overall similar wear characteristics for revision vs. posthumous retrievals[51]. Thirdly, we included only time *in situ* and mechanical axis limb alignment in our statistical models, which resulted in some of the inter-patient variability remaining unexplained, particularly as this data was not available for all patients. Other factors that could increase wear in some patients, but for which we did not have data, would be e.g. level of patient activity[52,53],

implant alignment parameters such as tibial rotation and posterior slope[24,54,55], or occasional lift-off during use[56,57].

Conclusion

This study adds to the small but important body of literature on volumetric wear rates of knee implants *in vivo*. Fixed-bearing implant design retrievals showed larger topside wear rates. Limb alignment had only a weak and non-significant effect on overall wear rates, but did affect the distribution of wear between the medial and lateral condyles. Further studies taking into account patient characteristics such as level of activity and other implant models are needed before a complete understanding of the variability in patient outcomes can be gained.

Acknowledgements

This work was supported by Empa and ETH Zurich. The authors would like to thank the Schulthess Clinic as well as Philippe Favre and Petra Koettig from Zimmer Biomet for providing access to the retrievals and CAD geometries. We also thank María Fernanda Álamos Salcedo and Pablo Alfonso Nunez Maldonado from Empa and Universidad Adolfo Ibáñez for performing 3D scan measurements.

References

1. Kandahari AM, Yang X, Laroche KA, et al. 2016. A review of UHMWPE wear-induced osteolysis: the role for early detection of the immune response. Bone Res. 4(1):16014.
2. Gallo J, Goodman SB, Konttinen YT, et al. 2013. Osteolysis around total knee arthroplasty: A review of pathogenetic mechanisms. Acta Biomater. 9(9):8046–8058.

3. Harman MK, DesJardins J, Benson L, et al. 2009. Comparison of polyethylene tibial insert damage from in vivo function and in vitro wear simulation. J. Orthop. Res. 27(4):540–548.

4. Harman M, Affatato S, Spinelli M, et al. 2010. Polyethylene insert damage in unicondylar knee replacement: A comparison of in vivo function and in vitro simulation. Proc. Inst. Mech. Eng. [H] 224(7):823–830.

5. Ngai V, Schwenke T, Wimmer MA. 2009. In-vivo kinematics of knee prostheses patients during level walking compared with the ISO force-controlled simulator standard. Proc. Inst. Mech. Eng. [H] 223(7):889–896.

6. Rawlinson JJ, Furman BD, Li S, et al. 2006. Retrieval, experimental, and computational assessment of the performance of total knee replacements. J. Orthop. Res. 24(7):1384–1394.

7. Abdel-Jaber S, Belvedere C, Leardini A, Affatato S. 2015. Wear simulation of total knee prostheses using load and kinematics waveforms from stair climbing. J. Biomech. 48(14):3830–3836.

8. Schwenke T, Wimmer MA, Schneider E, et al. 2005. Kinetics and wear of retrieved and simulator tested implants in TKA. In: 51st Annual Meeting of the Orthopaedic Research Society. p 1.

9. Dreyer MJ, Hosseini Nasab SH, Favre P, et al. 2023. Experimental and computational evaluation of knee implant wear and creep under in vivo and ISO boundary conditions. [cited 2023 May 12] Available from: http://medrxiv.org/lookup/doi/10.1101/2023.05.09.23289712.

10. Knowlton CB, Lundberg HJ, Wimmer MA, Jacobs JJ. 2020. Can a gait-dependent model predict wear on retrieved total knee arthroplasty components? Bone Jt. J. 102-B(6_Supple_A):129–137.

11. Oparaugo PC, Clarke IC, Malchau H, Herberts P. 2001. Correlation of wear debris-induced osteolysis and revision with volumetric wear-rates of polyethylene: A survey of 8 reports in the literature. Acta Orthop. Scand. 72(1):22–28.

12. Hood RW, Wright TM, Burstein AH. 1983. Retrieval analysis of total knee prostheses: a method and its application to 48 total condylar prostheses. J. Biomed. Mater. Res. 17(5):829–842.

13. Atwood SA, Currier JH, Mayor MB, et al. 2008. Clinical Wear Measurement on Low Contact Stress Rotating Platform Knee Bearings. J. Arthroplasty 23(3):431–440.

14. Knowlton CB, Bhutani P, Wimmer MA. 2017. Relationship of surface damage appearance and volumetric wear in retrieved TKR polyethylene liners. J. Biomed. Mater. Res. B Appl. Biomater. 105(7):2053–2059.

15. Cerquiglini A, Henckel J, Hothi HS, et al. 2018. Computed Tomography Techniques Help Understand Wear Patterns in Retrieved Total Knee Arthroplasty. J. Arthroplasty 33(9):3030–3037.

16. Rad EM, Laurent MP, Knowlton CB, et al. 2018. Linear Penetration as a Surrogate Measure for Volumetric Wear in TKR Tibial Inserts. In: Mihalko WM, Lemons JE, Greenwald AS, Kurtz SM, editors. Beyond the Implant: Retrieval Analysis Methods for Implant Surveillance. West Conshohocken, PA: ASTM International. p 75–92 [cited 2020 Jun 18] Available from: https://www.astm.org/doiLink.cgi?STP160620170119.

17. Teeter MG, Parikh A, Taylor M, et al. 2015. Wear and Creep Behavior of Total Knee Implants Undergoing Wear Testing. J. Arthroplasty 30(1):130–134.

18. Teeter MG, Milner JS, MacDonald SJ, Naudie DD. 2013. Manufacturing lot affects polyethylene tibial insert volume, thickness, and surface geometry. Proc. Inst. Mech. Eng. [H] 227(8):884–889.

19. Muratoglu OK, Perinchief RS, Bragdon CR, et al. 2003. Metrology to Quantify Wear and Creep of Polyethylene Tibial Knee Inserts. Clin. Orthop. 410:155–164.

20. Teeter MG, Naudie DDR, Bourne RB, Holdsworth DW. 2012. How Do CAD Models Compare With Reverse Engineered Manufactured Components for Use in Wear Analysis? Clin. Orthop. Relat. Res. 470(7):1847–1854.

21. Blunt LA, Bills PJ, Jiang X-Q, Chakrabarty G. 2008. Improvement in the assessment of wear of total knee replacements using coordinate-measuring machine techniques. Proc. Inst. Mech. Eng. [H] 222(3):309–318.

22. Jiang W, Ji C, Jin Z, Dai Y. 2018. CMM-Based Volumetric Assessment Methodology for Polyethylene Tibial Knee Inserts in Total Knee Replacement. Appl. Bionics Biomech. 2018:1–6.

23. Knowlton CB, Wimmer MA. 2012. An autonomous mathematical reconstruction to effectively measure volume loss on retrieved polyethylene tibial inserts. J. Biomed. Mater. Res. B Appl. Biomater. [cited 2019 Aug 8] Available from: http://doi.wiley.com/10.1002/jbm.b.32782.

24. Pourzal R, Cip J, Rad E, et al. 2020. Joint line elevation and tibial slope are associated with increased polyethylene wear in cruciate-retaining total knee replacement. J. Orthop. Res. 38(7):1596–1606.

25. Ashraf T, Newman JH, Desai VV, et al. 2004. Polyethylene wear in a non-congruous unicompartmental knee replacement: a retrieval analysis. The Knee 11(3):177–181.

26. Vandekerckhove P-JTK, Teeter MG, Naudie DDR, et al. 2017. The Impact of Coronal Plane Alignment on Polyethylene Wear and Damage in Total Knee Arthroplasty: A Retrieval Study. J. Arthroplasty 32(6):2012–2016.

27. Engh CA, Zimmerman RL, Hopper RH, Engh GA. 2013. Can Microcomputed Tomography Measure Retrieved Polyethylene Wear? Comparing Fixed-bearing and Rotating-platform Knees. Clin. Orthop. Relat. Res. 471(1):86–93.

28. McEwen HMJ, Barnett PI, Bell CJ, et al. 2005. The influence of design, materials and kinematics on the in vitro wear of total knee replacements. J. Biomech. 38(2):357–365.

29. Ahmad R, Senthil Kumar G, Katam K, et al. 2009. Significance of a “hot patella” in total knee replacement without primary patellar resurfacing. The Knee 16(5):337–340.

30. Palousek D, Omasta M, Koutny D, et al. 2015. Effect of matte coating on 3D optical measurement accuracy. Opt. Mater. 40:1–9.

31. Teeter MG, Brophy P, Naudie DD, Holdsworth DW. 2012. Comparison of micro-computed tomography and laser scanning for reverse engineering orthopaedic component geometries. Proc. Inst. Mech. Eng. [H] 226(3):263–267.

32. Zhou Q-Y, Park J, Koltun V. 2018. Open3D: A Modern Library for 3D Data Processing. [cited 2023 Jun 20] Available from: https://arxiv.org/abs/1801.09847.

33. R Core Team. 2023. R: A Language and Environment for Statistical Computing. Available from: https://www.R-project.org/.

34. Srivastava A, Lee GY, Steklov N, et al. 2012. Effect of tibial component varus on wear in total knee arthroplasty. The Knee 19(5):560–563.

35. Kim KT, Lee S, Ko DO, et al. 2014. Causes of Failure after Total Knee Arthroplasty in Osteoarthritis Patients 55 Years of Age or Younger. Knee Surg. Relat. Res. 26(1):13–19.

36. Pourzal R, Knowlton CB, Hall DJ, et al. 2016. How Does Wear Rate Compare in Well-functioning Total Hip and Knee Replacements? A Postmortem Polyethylene Liner Study. Clin. Orthop. Relat. Res. 474(8):1867–1875.

37. Taylor WR, Schütz P, Bergmann G, et al. 2017. A comprehensive assessment of the musculoskeletal system: The CAMS-Knee data set. J. Biomech. 65:32–39.

38. Dreyer MJ, Trepczynski A, Hosseini Nasab SH, et al. 2022. European Society of Biomechanics S.M. Perren Award 2022: Standardized tibio-femoral implant loads and kinematics. J. Biomech. 141:111171.

39. Morlock M, Schneider E, Bluhm A, et al. 2001. Duration and frequency of every day activities in total hip patients. J. Biomech. 34(7):873–881.

40. White PB, Ranawat AS, Ranawat CS. 2015. Fixed Bearings versus Rotating Platforms in Total Knee Arthroplasty. J. Knee Surg. 28(5):358–362.

41. Berry DJ, Currier JH, Mayor MB, Collier JP. 2012. Knee Wear Measured in Retrievals: A Polished Tray Reduces Insert Wear. Clin. Orthop. Relat. Res. 470(7):1860–1868.

42. Brandt J-M, MacDonald SJ, Bourne RB, Medley JB. 2012. Retrieval analysis of modular total knee replacements: Factors influencing backside surface damage. The Knee 19(4):306–315.

43. Currier JH, Currier BH, Abdel MP, et al. 2021. What factors drive polyethylene wear in total knee arthroplasty?: results of a large retrieval series. Bone Jt. J. 103-B(11):1695–1701.

44. Stoner KE, Nassif NA, Wright TM, Padgett DE. 2013. Laser Scanning as a Useful Tool in Implant Retrieval Analysis: A Demonstration Using Rotating Platform and Fixed Bearing Tibial Inserts. J. Arthroplasty 28(8):152–156.

45. Dennis DA, Komistek RD. 2005. Kinematics of Mobile Bearing Total Knee Arthroplasty. In: Bellemans J, Ries MD, Victor JMK, editors. Total Knee Arthroplasty. Berlin/Heidelberg: Springer-Verlag. p 126–140 [cited 2023 Jul 13] Available from: http://link.springer.com/10.1007/3-540-27658-0_20.

46. Thompson NW, Wilson DS, Cran GW, et al. 2004. Dislocation of the rotating platform after low contact stress total knee arthroplasty. Clin. Orthop. (425):207–211.

47. Smith CR, Vignos MF, Lenhart RL, et al. 2016. The Influence of Component Alignment and Ligament Properties on Tibiofemoral Contact Forces in Total Knee Replacement. J. Biomech. Eng. 138(2):021017.

48. Heller MO, Taylor WR, Perka C, Duda GN. 2003. The influence of alignment on the musculo-skeletal loading conditions at the knee. Langenbecks Arch. Surg. 388(5):291–297.

49. Halder A, Kutzner I, Graichen F, et al. 2012. Influence of Limb Alignment on Mediolateral Loading in Total Knee Replacement: In Vivo Measurements in Five Patients. J. Bone Jt. Surg. 94(11):1023–1029.

50. Vandekerckhove P-J, Lanting B, Bellemans J, et al. 2016. The current role of coronal plane alignment in total knee arthroplasty in a preoperative varus aligned population: an evidence based review. Acta Orthop Belg 82(1):129–42.

51. Wimmer M, Paul P, Haman J, et al. 2005. Differences in damage between revision and postmortem retrieved TKA implants. Trans. 51:1204.

52. Battaglia S, Taddei P, Tozzi S, et al. 2014. Toward the interpretation of the combined effect of size and body weight on the tribological performance of total knee prostheses. Int. Orthop. 38(6):1183–1190.

53. Schmalzried TP, Shepherd EF, Dorey FJ, et al. 2000. Wear Is a Function of Use, Not Time. Clin. Orthop. Relat. Res. 1976-2007 381:36–46.

54. Cerquiglini A, Henckel J, Hothi H, et al. 2018. 3D patient imaging and retrieval analysis help understand the clinical importance of rotation in knee replacements. Knee Surg. Sports Traumatol. Arthrosc. 26(11):3351–3361.

55. Johnston H, Abdelgaied A, Pandit H, et al. 2019. The effect of surgical alignment and soft tissue conditions on the kinematics and wear of a fixed bearing total knee replacement. J. Mech. Behav. Biomed. Mater. 100:103386.

56. Jennings LM, Bell CJ, Ingham E, et al. 2007. The influence of femoral condylar lift-off on the wear of artificial knee joints. Proc. Inst. Mech. Eng. [H] 221(3):305–314.

57. Todo S, Blunn GW, Harrison M, Freeman M a. R. 2003. The effect on wear of lift-off in total knee arthroplasty. Biomed. Mater. Eng. 13(3):231–234.